Hindawi
Mathematical Problems in Engineering
Volume 2022, Article ID 7682520, 12 pages
https://doi.org/10.1155/2022/7682520

Research Article

Influence of Vertical Downward Annulus Eccentricity on Steam-Water Two-Phase Flow Pressure Drop

Chuan Ma, Xiaoyan Liu, Haiqian Zhao, and Guangfu Cui

School of Mechanical Science and Engineering, Northeast Petroleum University, Daqing 163318, Heilongjiang, China

Correspondence should be addressed to Chuan Ma; mcnepu@nepu.edu.cn

Received 11 January 2022; Revised 24 February 2022; Accepted 3 March 2022; Published 7 April 2022

Academic Editor: Wei Liu

Concentric dual-tubing steam injection technique is one of the main methods to improve heavy oil recovery efficiency. From field data, it was discovered that hot fluid at high temperature and pressure caused steam injection casing to have elongation strain and "necking" eccentric buckling, and the eccentricity change affected the accurate prediction of steam-water two-phase flow pressure drop in the steam injection casing. This paper established a coupling model for the steam-water two-phase flow pressure drop in vertical downward eccentric annulus and the wellbore heat transfer and developed a mathematical model calculation program, to validate the accuracy of calculating the liquid holdup and pressure gradient of fully eccentric annulus. This revealed the influential law of eccentricity on the annulus steam-water two-phase pressure, dryness, and enthalpy value. The results indicated that when the eccentricity e increased from 0 to 1, the saturation pressure of steam at annulus wellbore bottom increased by 0.265 MPa, and the dryness and enthalpy value decreased by 8.54×10^{-3} and 11.22 kJ kg^{-1}, respectively. Compared to the concentric layout, the eccentrically arranged steam injection inner tube cannot promote the wet steam dryness at annulus wellbore bottom.

1. Introduction

The International Energy Agency (IEA) predicted [1] that the heavy oil resource occupies at least half of the world's exploitable oil resources, but its hyperviscosity and complex components make it harder to exploit. In order to increase heavy oil recovery efficiency, the oil fields have adopted the concentric steam flooding technique. However, in practical work condition, the heat strain from injected steam makes the steam injection inner tube have elongation strain and "necking" eccentric buckling, and the concentric dual-tubing steam injection will change to irregular eccentric dual-tubing steam injection. For the dual-tubing steam injection wellbores in oil fields, studying the influence of eccentricity on steam-water two-phase flow pressure drop is the key to accurately figuring out the wet steam pressure at annulus wellbore bottom.

The complex movement of the two-phase fluid in eccentric annulus wellbore makes it very difficult to predict the pressure drop of two-phase fluid. Gu et al. [2] used the semianalytical method to raise a model for predicting the steam-water mixture pressure in concentric dual-tubing steam injection wellbore, which mainly investigated the thermophysical properties of saturated steam and the wellbore heat loss. Based on the actual gas state equation as well as the mass, momentum, and energy conservation equations, Sun et al. [3–6] used the finite difference method and the iteration technique to disclose the change rules of on-way thermophysical property curves of multicomponent super-heated fluid, super-heated steam, and supercritical water in the concentric dual-tubing steam injection wellbore. Dong et al. [7] developed a model for the flowing and heat transfer of multicomponent hot fluids (including superheated water vapor, nitrogen, and carbon dioxide) in the concentric dual-tubing wellbore and parallel dual-tubing wellbore, taking the impact of wellbore temperature and pressure on its thermophysical properties into consideration. Li et al. [8] explored the influential law of steam injection well structure, steam injection proportion, and steam injection time on the physical properties of steam in the SAGD dual-tubing horizontal wellbore. On the basis of the flowing and heat transfer model of concentric dual-

tubing wellbore, Han et al. [9] considered the phase state variation of CO_2 and explored the pressure and temperature distribution of CO_2 in concentric casing. Wang and Su [10] got a numerical solution of pressure drop when the Bingham fluid moved axially in eccentric annulus, and obtained the empirical calculation formula through parametric regression, but they did not propose an empirical solution to the pressure drop formula applicable to the axial movement of Newtonian fluid. Ibarra et al. [11, 12] put forward a model for predicting the gas-liquid two-phase flow holdup and pressure drop at the slug flow state of horizontal concentric and fully eccentric tube sections, but this model was not universal for all flow patterns. In the field of concentric dual-tubing steam injection wellbore, the studies of wellbore two-phase pressure drop model are developing rapidly, while the calculation model of steam-water two-phase pressure drop in eccentric annulus still needs to be improved. To sum up, the method to solve the pressure drop of steam-water two-phase flow in vertical eccentric annulus has not been reported yet, and the influential law of eccentricity on the steam-water two-phase pressure drop within concentric dual-tubing steam injection wellbore is not clear.

Regarding the concentric dual-tubing steam injection wellbore, this paper built a coupling model for steam-water two-phase flow pressure drop in vertical eccentric annulus and wellbore heat transfer. Then, a calculation program was prepared to conduct simulation calculation of annulus water vapor pressure drop, which revealed the influential law of eccentricity on water vapor pressure, dryness, and enthalpy value in vertical annulus downcomer.

2. Model Establishment and Verification

2.1. Physical Model. Take concentric dual-tubing steam injection wellbore as an example. Due to the symmetry of cylindrical coordinate system, the physical model of vertical downward annulus was selected as shown in Figure 1. The wellbore structure includes steam injection inner tube, steam injection outer tube, insulated tubing, casing annular space (filled with low-pressure air), cement sheath, and formation from inside to outside. The water vapor at high temperature and pressure is injected into the steam injection casing at a certain flow velocity and dryness and dissipates heat to surrounding formation, which contains the calculation problem of steam-water two-phase flow pressure drop and the wellbore heat transfer problem. With the increase of well depth, the gas content of steam-water two-phase flow in the steam injection wellbore gradually decreases, and the flow patterns of the steam-water two-phase flow from well mouth to well bottom are annular flow, erratic flow, slug flow, and bubbly flow. Regarding the wellbore heat dissipation problem, at the initial steam injection period (less than 1 day), heat shall dissipate unstably in the wellbore, and both the steam injection time and the specific heat capacity of wellbore can greatly affect the heat flow density. When the steam injection time is more than 7 days, heat transfer can be deemed as stable inside the wellbore. For the steam injection wellbore using steam flooding technique, heat transfers stably; for the wellbores using steam stimulation techniques such as closing-in, well completion, and well soaking, the heat transfer should be transient. The on-way pressure of water vapor in the wellbore bears the impact from flow pattern and dryness at the same time. By dividing the wellbore into several infinitesimal sections and analyzing the radial heat transfer process of each section, the wellbore-formation coupled radial heat transfer includes condensation heat transfer of the steam in steam injection casing, heat conduction of insulated tubing, free convection and radiation heat exchange of the casing annular space, heat conduction of cement sheath, and transient heat conduction of formation.

Eccentricity is one of the structural parameters of annulus tube, which represents the offset distance from inner tube center to outer tube center [13]. See its definition in (1), and eccentricity value changes within 0~1. Figure 2 shows the cross-sectional view of annulus tube under a certain annulus tube diameter ratio when the eccentricity is 0, 0.5, and 1.

$$e = \frac{2\ DBC}{D_C - D_T}, \tag{1}$$

In the above equation, e is the eccentricity of annulus tube, dimensionless; D_C is the outer diameter of tubing, in meters; D_T is the inner diameter of steam injection casing, in meters; and DBC is the distance between inner tube center and outer tube center, in meters.

2.2. Mathematical Model. The coupling model for the steam-water two-phase flow pressure drop in vertical eccentric annulus and the wellbore heat transfer consists of two parts: pressure drop and wellbore heat transfer. By virtue of the relationship between water vapor's saturation temperature and saturation pressure, the wellbore heat dissipation was coupled with the pressure drop, and the calculation of the water vapor pressure in eccentric annulus was coupled with the calculation of dryness and temperature.

To simplify the mathematical model, we made the following assumptions: (1) heat transfer from the wellbore to outer edge of cement sheath is at a one-dimensional steady state, and heat transfer from cement sheath to formation is at a one-dimensional nonsteady state, while the axial heat transfer of water vapor along well depth direction is ignored; (2) the heat conductivity coefficient of the formation is deemed as a constant; (3) the water vapor is at a one-dimensional two-phase steady flowing state; (4) the heat dissipation of isolated tubing coupling is ignored; (5) the wellbore-formation coupling heat transfer condition is constant heat flow; and (6) the boundary of the heat-affected zone of the formation is an insulated boundary.

The pressure drop calculation model gave preference to the Caetano prediction model for steam-liquid two-phase flow pressure drop in vertical downward eccentric annulus and the drift-flux model based on Bhagwat's sectional void fraction correlation [13].

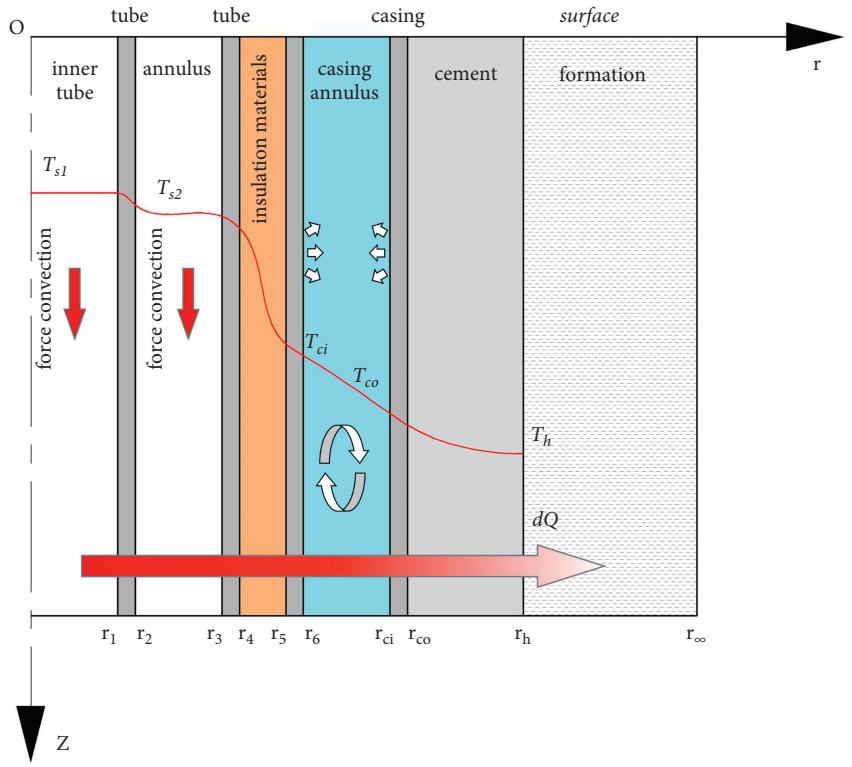

Figure 1: Physical model of the concentric steam flooding wellbore system.

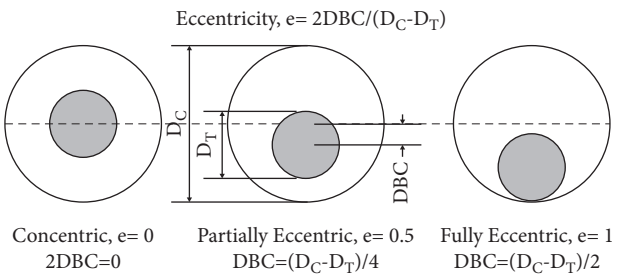

Figure 2: Annulus tube structure.

2.2.1. Optimal Pressure Drop Model

(1) Calculation of sectional void fraction [13]

Calculation of distribution coefficient C_0 is as below:

$$C_0 \approx 1 + \left(0.2 - 0.2\sqrt{\rho_g/\rho_l}\right) \cdot \left[(2.6 - \beta)^{0.15} - \sqrt{f_{tp}}\right](1 - x)^{1.5}. \quad (2)$$

Calculation of drift velocity v_{gj} is as below:

$$v_{gj} = (0.35 \sin\theta + 0.45\cos\theta)\sqrt{gD_h(\rho_l - \rho_g)/\rho_l} \cdot (1 - \alpha)^{0.5} C_2 C_3 C_4. \quad (3)$$

Calculation of sectional void fraction α is as below:

$$\alpha = \frac{\beta}{C_0 + v_{gj}/v_m}, \qquad H_L = 1 - \frac{\beta}{C_0 + \left(v_{gj}/v_m\right)}. \quad (4)$$

In the above equations, C_2, C_3, and C_4 are the correction coefficients in drift velocity calculation; f_{tp} is the friction factor; β is the volumetric void fraction; α is the sectional void fraction; H_L is the liquid holdup; the detailed calculation of above dimensionless parameters is shown in the literature [13]; ρ_g is the gas phase density, in kg•m^{-3}; ρ_l is the liquid phase density, in kg•m^{-3}; x is the dryness; and D_h is the hydraulic diameter, in meters.

(2) Calculation of pressure gradient

Based on the previous flow pattern division and transition criterion theories for vertical annulus gas-liquid two-phase flow [14, 15], the flow patterns are divided into annular flow, slug flow, and bubbly flow. The transition condition from slug flow to annular flow is the sectional void fraction $\alpha = 0.7$, and the transition condition from bubbly flow to slug flow is $\alpha = 0.2$ under concentric annulus. The transition condition from slug flow to annular flow is the sectional void fraction $\alpha = 0.8$, and the transition condition from bubbly flow to slug flow is $\alpha = 0.15$

under fully eccentric condition. Figure 3 shows the flow pattern of annulus gas-fluid two-phase flow under fully eccentric condition. The division of gas-liquid two-phase flow pattern of fully eccentric annulus is similar to that of concentric annulus, while the existence of eccentric annulus breaks the symmetric distribution characteristics of bubbles along tube center. In a wide annular space, the local sections have a higher void fraction. In a narrow annular space, the local void fraction is lower. This makes the transition boundary from bubbly flow to slug flow move to the direction with decreasing average sectional void fraction, untimely forming the slug flow.

In view of the complexity of annular channel, the circular tube pressure drop theory expressed in form of equivalent hydraulic diameter cannot concretely describe the structural feature and flowing characteristic of annulus tube. Therefore, the Caetano annulus pressure drop correlation was introduced; see the calculation model in (5)~(7):

(a) The slug flow is as follows:

$$\frac{dp}{dz} = \rho_m g \frac{L_{LS}}{L_{SU}} - \lambda \frac{\rho_m v_m^2}{2D_h} \frac{L_{LS}}{L_{SU}} + \rho_m v_m dv_m, \tag{5}$$

$$\rho_m = \alpha\rho_g + (1-\alpha)\rho_l, \quad \mu_m = \alpha\mu_g + (1-\alpha)\mu_l, \quad h_m = xh_g + (1-x)h_l. \tag{6}$$

In the above equations, λ is the friction resistance coefficient, dimensionless; L_{LS} is the liquid slug length, in meters; and L_{SU} is the length of slug unit, in meters [16]. The presentation form of two-phase mixture parameters is shown in (8), where ρ_m is the density of two-phase mixture, in kg•m^{-3}; α is the sectional void fraction, dimensionless; μ_m is the viscosity of two-phase mixture, in Pa•s; v_m is the velocity of two-phase mixture, in m•s^{-1}; h_m is the enthalpy value of two-phase mixture, in kJ•kg^{-1}; μ_g is the viscosity coefficient of gas phase, in Pa•s; μ_l is the viscosity coefficient of liquid phase, in Pa•s; h_l is the enthalpy value of liquid phase, in kJ•kg^{-1}; and h_g is the enthalpy value of gas phase, in kJ•kg^{-1}.

(b) The annular flow is as follows:

$$\left(\frac{dp}{dz}\right)_{\text{core}} = \rho_{\text{core}} g - \tau_{CI}\frac{S_{CI}}{A_{\text{core}}} - \tau_{TI}\frac{S_{TI}}{A_{\text{core}}}. \tag{7}$$

Under a stable gas-liquid interface of annular flow, the pressure drops are equal at gas core, inner tube's liquid film, and outer tube's liquid film, and the pressure drop at gas core represents the pressure drop of gas-liquid two-phase flow. The drift-flux model is based on the idea of weighted average to figure out the mean value of two-phase flow parameters distributed along the cross section. Thus, the calculated value of the above sectional void fraction, as well as the calculated pressure, temperature, dryness, and steam enthalpy values, is a mean value distributed along the cross section.

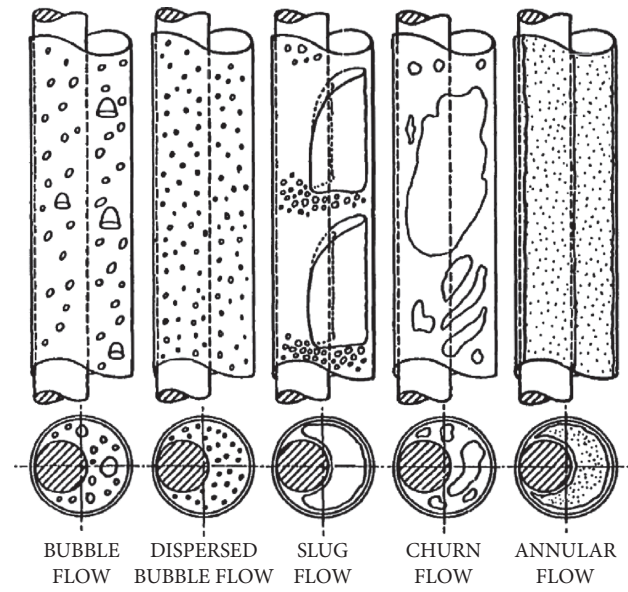

Figure 3: Flow pattern diagrams of fully eccentric annular upward tube, Caetano et al. [16].

(b) The annular flow is as follows:

Under a stable gas-liquid interface of annular flow, the pressure drops are equal at gas core, inner tube's liquid film, and outer tube's liquid film, and the pressure drop at gas core represents the pressure drop of gas-liquid two-phase flow. The drift-flux model is based on the idea of weighted average to figure out the mean value of two-phase flow parameters distributed along the cross section. Thus, the calculated value of the above sectional void fraction, as well as the calculated pressure, temperature, dryness, and steam enthalpy values, is a mean value distributed along the cross section.

Under a stable gas-liquid interface of annular flow, the pressure drops are equal at gas core, inner tube's liquid film, and outer tube's liquid film, and the pressure drop at gas core represents the pressure drop of gas-liquid two-phase flow. The drift-flux model is based on the idea of weighted average to figure out the mean value of

two-phase flow parameters distributed along the cross section. Thus, the calculated value of the above sectional void fraction, as well as the calculated pressure, temperature, dryness, and steam enthalpy values, is a mean value distributed along the cross section.

(3) Calculation of tubing/casing liquid film thickness ratio

The plane angle toward the tubing wall is one of the main parameters to solve the tubing/casing liquid film thickness ratio in eccentric annular structure. Caetano pointed out that solving the plane angle in eccentric annulus is different from that in concentric annulus. See the calculation of plane angle in (8), where e is the eccentricity, dimensionless; K is the radius ratio of annulus tube, dimensionless, $K = D_T/D_C$; and W_T' is the plane angle toward the tubing wall, in rad. The symbol denotes the mean values along the annular cross section. Since (8) has no analytical solution, the approximate solution can only be obtained by using numerical algorithm such as the complexification Simpson rule.

$$\langle W_T' \rangle = \frac{1}{\pi\left(1 - K^2\right)} \int_0^{\pi} \left[8a^2 \sin^{-1}\left(\frac{K}{2a}\right) + 2K\sqrt{4a^2 - K^2} - K^2\ \pi \right] d\theta,$$
$$a = \frac{e}{2}(1 - K)\cos\ \theta + \frac{1}{2}\sqrt{e^2(1 - K)^2\left(\cos^2\ \theta - 1\right) + 1}. \quad (8)$$

2.2.2. Quasi-Stable Heat Transfer Model for Dual-Tubing Steam Injection Wellbore

(1) The formula of dryness gradient

$$\frac{dx}{dz} = -\frac{1}{h_g - h_l}\left[\frac{1}{W}\frac{dQ}{dz} + \left(x\frac{dh_g}{dT} + (1 - x)\frac{dh_l}{dT}\right)\frac{dT}{dP}\frac{dP}{dz} - \frac{v_m v_{sg}}{P}\frac{dP}{dz} + g\right]. \quad (9)$$

(2) The formula of heat transfer coefficient from inside the wellbore to outer edge of cement sheath

By working out the wellbore structural data in relevant literature [17], the heat resistance of thermal insulation layer, casing annulus layer, and cement annulus accounts for 99.68% of the heat resistance of wellbore inner layer, in which the steel tube and condensation heat transfer resistance are ignored. The simplified heat transfer coefficient from inside the wellbore to cement annulus is shown as follows:

$$U = \left(\frac{r_2}{\lambda_{ins}}\ln\frac{r_5}{r_4} + \frac{r_2}{(h_c + h_r)r_6} + \frac{r_2}{\lambda_{cem}}\ln\frac{r_{cem}}{r_{co}}\right)^{-1}. \quad (10)$$

(3) Condition of wellbore-transformation coupling heat transfer

$$dQ = 2\pi r_2\left[U\left(T_{S1} - T_h\right)\right]dz = \frac{2\pi\lambda_e\left(T_h - T_e\right)}{f(t)}dz\ . \quad (11)$$

In (11), the left side of the equation denotes the quasi-stable heat transfer from wellbore to outer edge of cement annulus, and the right side of the equation denotes the transient heat conduction of the formation. This can be interpreted as follows: the heat flow density inside the wellbore is equal to that at the formation contact boundary.

In the above equation, λ_{ins} is the hat conductivity coefficient of thermal isolation materials, in $W \bullet m^{-1} K^{-1}$; λ_{cem} is the heat conductivity coefficient of cement annulus, in $W \bullet m^{-1} K^{-1}$; λ_e is the heat conductivity coefficient of the formation, in $W \bullet m^{-1} K^{-1}$; h_r is the radiation heat exchange coefficient of casing annular layer, in $W \bullet m^{-2} K^{-1}$; h_c is the natural-convection heat transfer coefficient of casing annular layer, in $W \bullet m^{-2} K^{-1}$; W is the mass velocity, in $kg \bullet s^{-1}$; Q is the heat flow density, in $W \bullet m^{-2}$; v_{sg} is the apparent gas phase velocity, in $m \bullet s^{-1}$; v_m is the flow velocity of two-phase mixture, in $m \bullet s^{-1}$. T_h is the temperature of the outer edge of cement annulus, in K; T_e is the temperature of the formation, in K; T_{S1} is the steam temperature in the steam injection inner tube, in K; and $f(t)$ is the formation thermal conduction time function, dimensionless.

(4) Differential equation of the formation's transient thermal conduction

The differential equation of one-dimensional radial formation transient thermal conduction can be interpreted mathematically as below:

$$\frac{\partial^2 t}{\partial r^2} + \frac{1}{r}\frac{\partial t}{\partial r} = \frac{1}{\alpha}\frac{\partial t}{\partial \tau}. \quad (12)$$

The initial condition is as follows:

$$\text{When } \tau = 0: \quad t_e = t_0 + mz. \quad (13)$$

The boundary condition is as follows:

$$\text{When } r = r_\infty: \quad \frac{\partial t}{\partial r} = 0,$$
$$r = r_h: \quad dQ = -2\pi r_h dz\ \lambda_e \frac{\partial t}{\partial r}\Big|_{r=r_h}. \quad (14)$$

In the above equations, t is the formation temperature distribution, $t = f(\tau, r)$, in K; t_0 is the surface temperature, in K; m is the surface temperature

gradient, in K m^{-1}; λ_e is the formation thermal conductivity coefficient, in W•m^{-1} K^{-1}; and α is the formation thermal diffusion coefficient, in m^2 s^{-1}.

The solution of the differential equation of formation transient thermal conduction is detailed in literature [17], in which the formation transient thermal conduction function $f(t)$ has taken the Chiu semi-empirical correlation for reference.

2.3. Model Validation

2.3.1. Validation of Liquid Holdup H_L. The relationship of liquid holdup H_L and sectional void fraction α is as follows: $H_L = 1 - \alpha$. The 49 groups of experimental data of fully eccentric annulus are selected [16, 18], and the predicted and measured liquid holdup values of air-water two-phase flow in vertical upward fully eccentric annulus are compared in Figure 4. It can be seen from Figure 4 that *MRD* and *Std* are the average relative error and standard deviation, respectively. On account of that, the void fraction is higher and the liquid holdup is lower in the annular flow condition, so it is suitable to measure the accurate calculation of liquid holdup by using absolute error. Therein, the average relative error of bubbly flow and slug flow is −2.6%. Except several data points falling outside the error band of 20%, 95% of the data points fall within the 20% error band, and 87% of the data points have an error less than 10%; the average absolute error of annular flow is 0.0226. The results indicate that the predicted liquid holdup value fits well with the Caetano measured value and that the Bhagwat correlation can meet the allowable error in engineering calculation of liquid holdup.

$$\begin{aligned} \mathrm{MRD}\,(\%) &= \frac{1}{N}\sum_{i=1}^{N}\frac{x_{\mathrm{predicted}} - x_{\mathrm{measured}}}{x_{\mathrm{measured}}}, \\ \mathrm{Std}\,(\%) &= \sqrt{\frac{1}{N}\sum_{i=1}^{N}\left(x_{\mathrm{predicted}} - x_{\mathrm{measured}}\right)^2}. \end{aligned} \tag{15}$$

Compared to concentric annulus, the existence of eccentric inner tube can lead to a smaller local liquid holdup in wider annular space, a larger local liquid holdup in narrower gap, and a greater impact on average sectional liquid holdup from annulus eccentricity. This is also the reason for the prediction error of liquid holdup.

2.3.2. Validation of Pressure Gradient. In Figure 5, the predicted value and measured value of pressure drop of air-water two-phase flow in vertical upward fully eccentric annulus were compared [18]. The work condition of Caetano experiment is as follows: inner diameter of 0.0422 m, outer diameter of 0.0762 m, temperature of 28.7°C, system pressure of 0.315 MPa, and air-water two-phase flow of vertical upward fully eccentric annulus in adiabatic work condition. It can be seen from Figure 5 that the average relative error of pressure gradient is −21.15%, and the model can predict the pressure drop of eccentric annulus, which verifies the accurate calculation of pressure drop in eccentric annulus model.

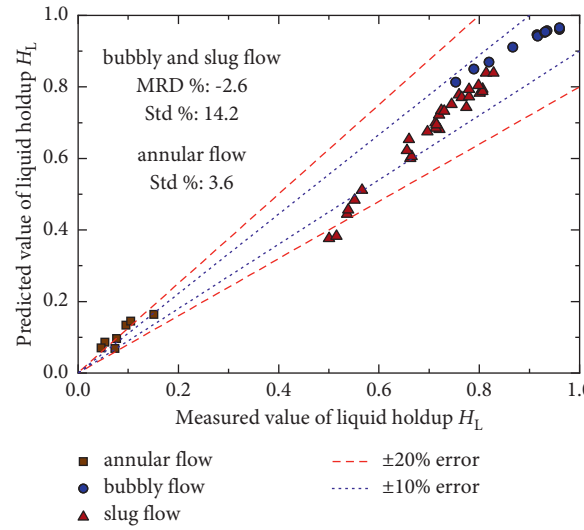

Figure 4: Comparison of predicted value and measured value of liquid holdup of fully eccentric annulus.

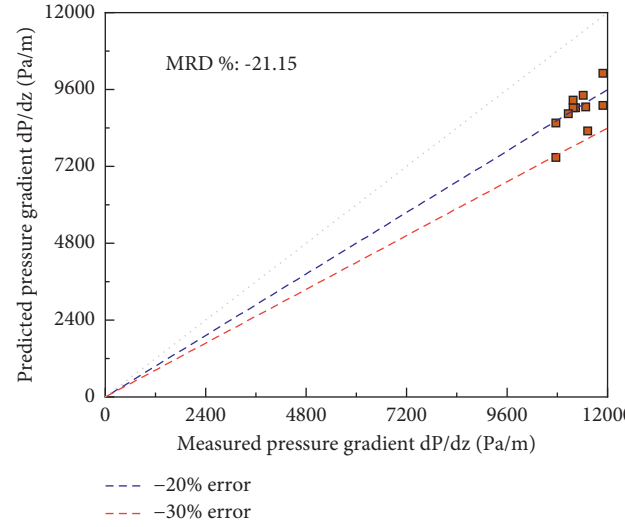

Figure 5: Comparison of predicted value and measured value of pressure gradient of fully eccentric annulus.

Some of the prediction errors are caused by friction factors f_{CI} and f_{TI}. The tubing/casing liquid film thickness ratio reduces, which changes the Fanning friction factors, thereby affecting the frictional pressure drop. The existence of eccentric inner tube breaks the symmetry of bubble distribution in gas-liquid two-phase flow, inevitably changing the friction factor of eccentric annulus. Recently, an empirical formula for friction factor of gas-liquid two-phase flow in the fully eccentric annulus with a wide range of Reynolds numbers is still lacking, so only the empirical formula for friction factor of concentric annulus can be used to approximately calculate the frictional pressure drop of fully eccentric annulus.

The above research contents verify the accuracy of predicting liquid holdup and pressure drop through the pressure drop calculation model for gas-liquid two-phase flow in eccentric annulus. The calculation model can satisfy the allowable error in the engineering calculation of liquid holdup and pressure gradient.

3. Influential Analysis of Eccentricity on the Pressure Drop of Gas-Liquid Two-Phase Flow in Vertical Annulus

The basic parameters of dual-tubing steam injection wellbore are shown in Table 1 [16]. A simulation analysis was made on the influential rule of eccentricity on the water vapor pressure in vertical annulus, as well as the change law of water vapor's on-way pressure in annulus tube under a certain eccentricity.

3.1. Influential Law of Eccentricity on the Water Vapor On-Way Pressure in Vertical Annulus. In an annular geometric structure with the eccentricity $e = 0/0.5/1$, the influence of eccentricity on the water vapor on-way pressure of wellbore annulus is demonstrated in Figure 6.

As can be seen from Figure 6, when the well depth is 1000 m, due to the superposition of on-way frictional pressure drop in the wellbore, the influence of eccentricity on the steam pressure at wellbore bottom is more obvious in comparison with on-way pressure. With the increase of depth, the water vapor pressure along the wellbore annulus decreases gradually, and the higher the eccentricity, the greater the pressure along the wellbore annulus. The steam pressure at well bottom is the key to steam flood power, so it is necessary to make in-depth analysis of it.

3.2. Influential Law of Eccentricity on the Water Vapor Pressure at Vertical Annulus Bottom. When the dryness of injected steam is greater than 0.2, the steam-water two-phase flow pattern is determined as annular flow. See Figure 7 for the influence of eccentricity on the steam-water mixture pressure and frictional pressure drop at well bottom. See Figure 8 for the tubing/casing liquid film thickness ratio at well bottom under different eccentricity.

Figure 7 shows that the eccentricity e of vertical annulus increases from 0 to 1, causing the water vapor pressure at well bottom to increase by 0.265 MPa. Apparently, the frictional pressure drop decreases by 31.42 kPa, but actually, the tubing/casing liquid film thickness ratio reduces by 0.099 as shown in Figure 8. This changes the wet perimeters S_{CI} and S_{TI} of gas-liquid interface at tubing side and casing side as well as the Fanning friction factors f_{CI} and f_{TI}, thereby affecting the frictional pressure drop. From concentric to fully eccentric annulus structure, the frictional pressure drop at well bottom is lowered. Some scholars [10, 11] also obtained similar results through experiments. Ibarra et al. [11] considered that the frictional pressure drop of concentric annulus is larger than that of fully eccentric annulus and completed its validation through experiment. Similarly, Wang and Su [10] studied the calculation of the flowing pressure drop of Bingham fluid in eccentric annulus and discovered that the increase of eccentricity can bring down the frictional pressure drop of annulus fluid, and the larger the radius ratio K of annulus is, the greater the frictional pressure drop decreases.

When the eccentricity becomes larger, the sectional void fraction at annulus bottom turns lower. The decreasing trend of the section gas holdup is similar to the liquid film thickness ratio of the casing shown in Figure 8. When the mass velocity is constant, a lowered sectional void fraction can cause the density of steam-water two-phase mixture to increase, the flowing velocity of two-phase mixture to decrease, the interaction of gas core and wall liquid film in an annular flow to weaken, and the frictional pressure drop to become smaller. The structural change of annulus has little impact on the wellbore heat transfer, and the influence of eccentricity on the wellbore on-way heat loss and dryness can be ignored. It is known from Figure 7 that, compared to frictional pressure drop, the dynamic pressure at well bottom is smaller than the frictional pressure drop by an order of magnitude. This indicates that the frictional pressure drop is the main reason for the change of steam saturation pressure and temperature at well bottom.

From the above analysis, the results express the following: when the eccentricity e increases from 0 to 1, the wet steam saturation pressure at annulus bottom rises by 0.265 MPa, the dryness decreases slightly by 8.54×10^{-3}, the enthalpy value decreases by 11.22 kJ kg^{-1}, and the wellbore heat loss basically remains unchanged. Therefore, for a concentric dual-tubing steam injection wellbore, the scheme is theoretically infeasible to promote the wet steam dryness at annulus bottom by an eccentric arrangement of steam injection inner tube. Increasing the eccentricity can slightly reduce the wet steam dryness at annulus bottom, and a concentric arrangement of steam injection inner tube can help to obtain a higher dryness at annulus bottom. Starting with the wellbore insulation effect, increasing the thermal resistance of insulated tubing, improving tubing annulus, and promoting the insulation performance of tubing coupling can effectively improve the steam dryness at wellbore bottom. Eccentrically arranged inner tube can raise the wet steam saturation pressure at annulus bottom and improve steam flooding capability.

3.3. Change Rules of On-Way Pressure of Annulus Wet Steam under Constant Eccentricity. When the eccentricity $e = 0.5$, the change of steam on-way pressure in eccentric annulus is shown in Figure 9.

Figure 9 shows that the steam on-way pressure decreases quickly with the increase of well depth. In the figure, the dotted line represents the minimal apparent gas phase velocity v_{sgcr} required in the transition of water vapor from erratic flow to annular flow. For a vertical upward tube, the physical significance of critical apparent gas velocity is the minimal apparent gas velocity required by the liquid drop carried in the gas core to move upward, and its value is determined by the balance between the gravity and drag force of the largest and most stable liquid drop in the gas core. For a vertical

Table 1: Basic wellbore parameters.

Basic parameters	Value, unit	Basic parameters	Value, unit
Inner diameter of steam injection inner tube (r_1)	0.027 m	Thermal conductivity of tubing and casing (λ_{tube}, λ_{cas})	45W•m^{-1} K^{-1}
Outer diameter of steam injection inner tube (r_2)	0.038 m	Thermal conductivity of insulation materials (λ_{ins})	0.076 W•m^{-1} K^{-1}
Inner diameter of steam injection annulus tube (r_3)	0.062 m	Thermal conductivity of cement annulus (λ_{cem})	0.933 W•m^{-1} K^{-1}
Outer diameter of steam injection annulus tube (r_4)	0.073 m	Thermal conductivity of formation (λ_e)	1.7305 W•m^{-1} K^{-1}
Inner diameter of insulated tubing (r_5)	0.1003 m	Thermal diffusion coefficient of formation (α_e)	1.75×10^{-6} m s^{-2}
Outer diameter of insulated tubing (r_6)	0.1143 m	Surface temperature gradient ($T_{gradient}$)	0.03 K•m^{-1}
Inner diameter of casing (r_{ci})	0.1594 m	Surface temperature ($T_{surface}$)	302.15 K
Outer diameter of casing (r_{co})	0.1778 m	Tubing outer wall blackness (ε_6)	0.8
Outer diameter of cement annulus (r_h)	0.2410 m	Casing inner wall blackness (ε_{ci})	0.1

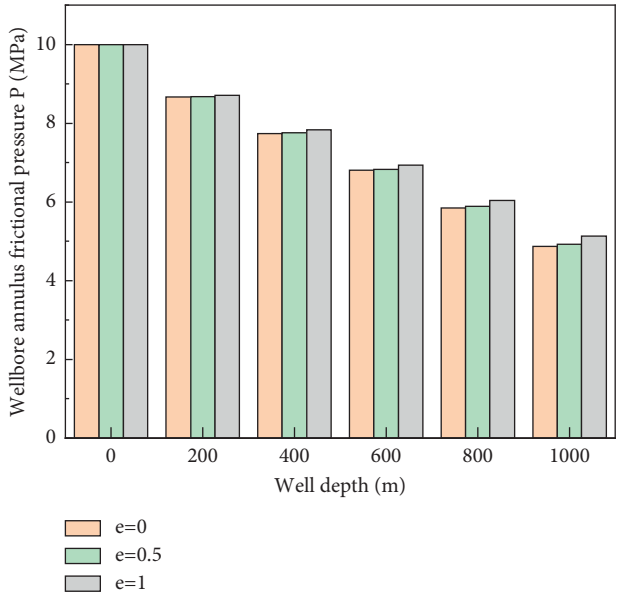

Figure 6: Influential law of eccentricity on the water vapor on-way pressure in annulus tube.

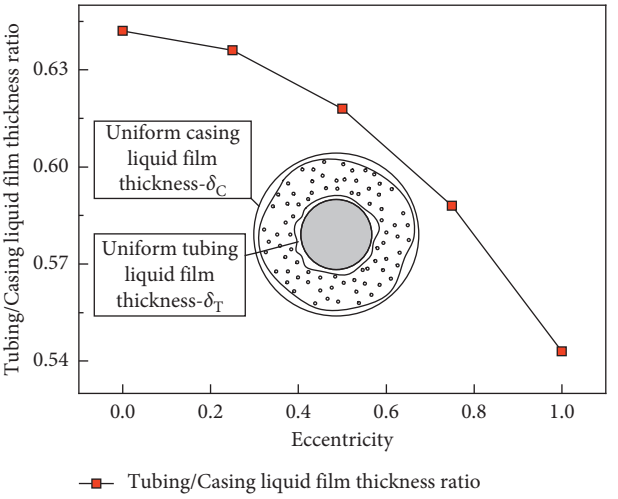

Figure 8: Tubing/casing liquid film thickness ratio at well bottom under different eccentricity.

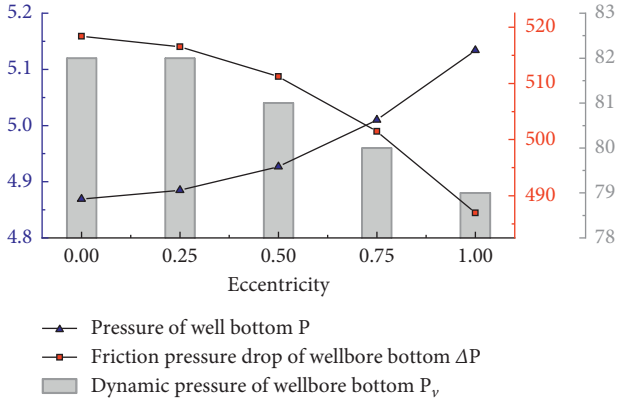

Figure 7: Influence of eccentricity on the steam-water mixture pressure and frictional pressure drop at well bottom.

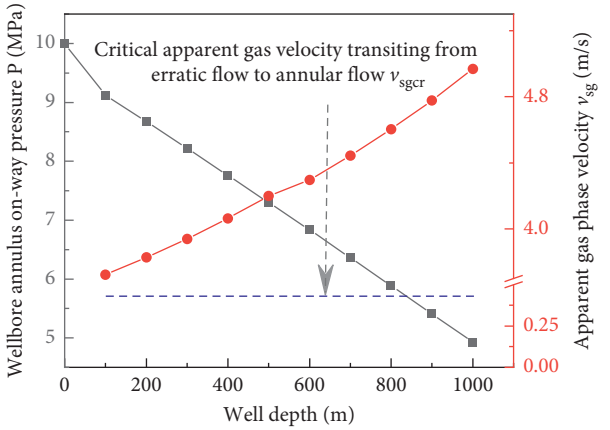

Figure 9: Change rule of steam on-way pressure in eccentric annulus.

downward tube, the directions of the gravity and drag force borne by the liquid drops carried are all downward, making it hard to form falling film, whose critical apparent gas velocity v_{sgcr} is lower than that of an upward tube.

In Figure 9, the critical apparent gas velocity v_{sgcr} is 0.433 m s^{-1}, the apparent gas velocity at annulus inlet v_{sg} is 3.72 m s^{-1}, and the water vapor flow pattern has already turned into annular flow. When the well depth increases, the apparent gas velocity of water vapor continue to rise to 4.97 m s^{-1}. At this time, the water vapor flow pattern transits to a fully developed annular flow. The friction effect between gas core and wall liquid film becomes larger, frictional pressure drop takes a bigger and bigger proportion in total pressure drop, and the dynamic pressure increases by about 32%, as shown in Figure 10. Thus, the steam on-way pressure declines dramatically with well depth.

As shown in Figure 10, because the water vapor flow pattern gradually transits to a fully developed annular flow, the on-way frictional pressure drop of steam quickly rises at the well depth of 500 m, fluctuates up and down within the well depth of 600~1000 m, and shows an extreme value in this depth range. These are caused by the on-way change of shear stress of gas core and steam injection inner/outer tube liquid film, and the friction factor of gas core and wall falling film is the main factor. When the eccentricity $e = 0.5$, the on-way distribution law of the frictional shear stress between gas core and the inner and outer wall liquid film of steam injection annulus (as shown in Figure 11) is similar to the on-way frictional pressure drop as shown in Figure 10.

The solid lines in Figure 11 represent the on-way distribution of shear stress between the inner wall liquid film of steam injection annulus and gas core, and the dotted lines represent the on-way distribution of shear stress between the outer wall liquid film of steam injection annulus and gas core. It is known from Figure 11 that, whether the annular geometric structure is concentric or eccentric with $e = 0.5$, the shear stress between the inner wall liquid film of steam injection annulus and gas core is always larger than that of the outer wall of steam injection annulus; that is to say, $\tau_{TI} > \tau_{CI}$. Caetano found out by experiment that, under annular flow condition, the tubing wall liquid film δ_T is thinner than casing wall liquid film δ_C. The fact that the tubing/casing liquid film thickness ratio is less than 1 (Figure 8) also conforms to this conclusion, which makes the shear stress between the inner wall liquid film of steam injection annulus and gas core always larger than that of the outer wall of steam injection annulus. It is precisely because the shear stress between the inner wall liquid film of steam injection annulus and gas core τ_{TI} is larger, in the annular flow, the gas core exerts a greater drag force on the liquid falling film of annulus inner wall, and more small droplets are carried, causing the liquid film of annulus inner wall to become thinner. In Figure 11, take well depth of 400 m as an example; as the eccentricity increases from 0 to 0.5, the shear stress between the annulus inner wall liquid film and gas core τ_{TI} reduces by 1.35 Pa, and the shear stress between the annulus outer wall liquid film and gas core τ_{CI} rises by 0.316 Pa. This indicates that the eccentricity exerts different impact on the shear stress between gas core and annulus

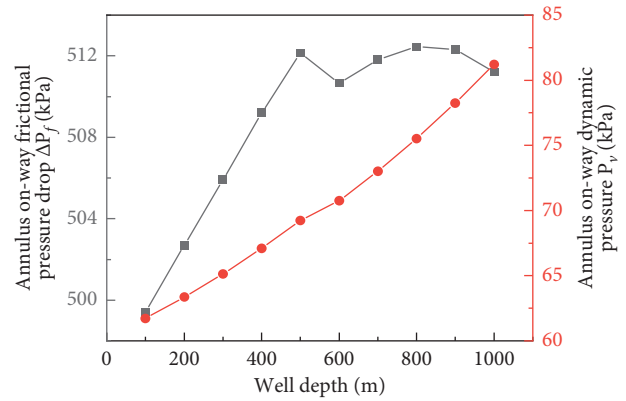

Figure 10: Steam on-way frictional pressure drop and dynamic pressure in eccentric annulus.

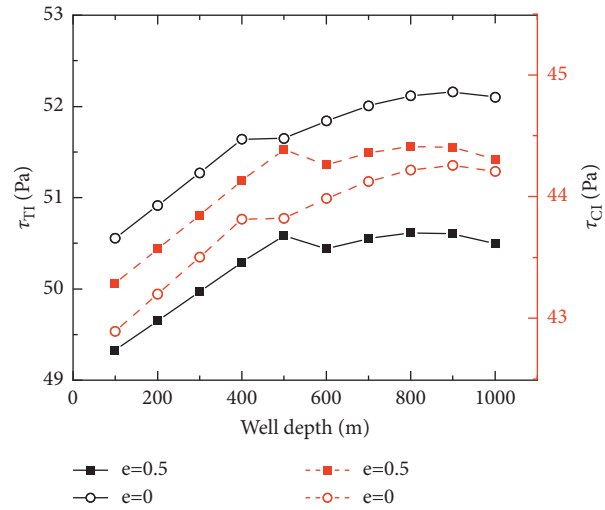

Figure 11: On-way distribution of frictional shear stress between gas core and casing inner/outer walls.

inner/outer wall liquid film. However, the change rule of the shear stress between liquid film and gas core with well depth displays a rapid rise at first, followed by a steady change ($e = 0$) or a slight down-fluctuation ($e = 0.5$), and finally a gentle rise ($e = 0$) or the appearance of an extreme value ($e = 0.5$).

In order to reveal the influence law of pipe diameter, mass flow rate, and steam injection dryness on wet steam pressure at the bottom of annulus pipe under concentric and certain eccentricity conditions, the analysis of influencing factors of wet steam pressure at the bottom of annulus pipe under concentric and eccentricity conditions will be carried out below.

3.4. Influence of Steam Injection Inner Tube Diameter on Wet Steam Pressure at Annulus Bottom. The influence of steam injection inner tube diameter on the wet steam pressure at annulus bottom under concentric and given eccentricity conditions is demonstrated in Figure 12. The histogram ordinate denotes the wet steam saturation pressure at well bottom, and the ordinate of point plot represents the

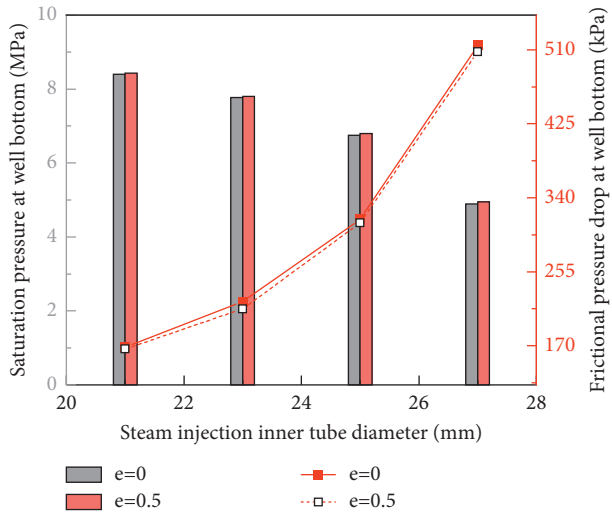

Figure 12: Influence of steam injection inner tube diameter on the wet steam pressure at well bottom.

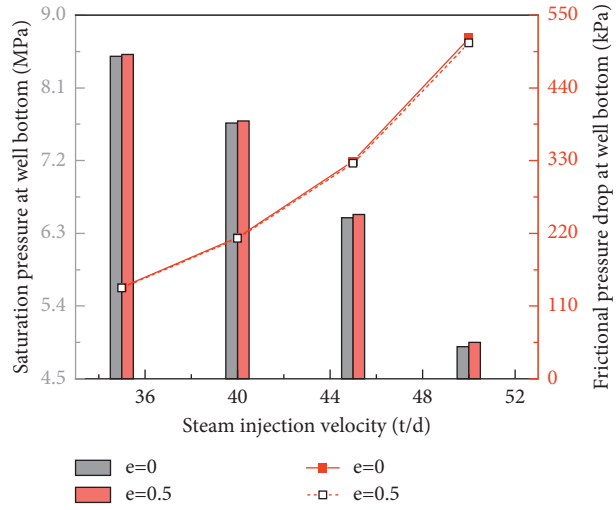

Figure 13: Influence of steam injection velocity on wet steam pressure at annulus bottom.

frictional pressure drop at well bottom. In Figure 12, when the eccentricity remains unchanged, as the inner tube diameter rises, the wet steam saturation pressure at annulus bottom declines, and the frictional pressure drop of wet steam increases. Therefore, under a constant tube diameter, the eccentricity has little impact on the wet steam saturation pressure and frictional pressure drop at well bottom.

From the results of Figure 7, we can know that an increased eccentricity can result in a slight rise in the wet steam saturation pressure at well bottom and a slight decline in frictional pressure drop. Take the steam injection inner tube radius of 21 mm as an example; as the eccentricity rises by 0.5, the wet steam frictional pressure drop at well bottom reduces by about 2.3 kPa, which basically will not change the wet steam saturation pressure at well bottom by an order of magnitude of 1 MPa. Accordingly, the influence of the eccentricity on the wet steam saturation pressure and frictional pressure drop at annulus bottom can be ignored.

3.5. Influence of Steam Injection Outer Tube's Mass Flow Rate on the Wet Steam Pressure at Annulus Bottom. The influence of steam injection velocity on wet steam pressure at annulus bottom is shown in Figure 13. The histogram ordinate denotes the wet steam saturation pressure at well bottom, and the ordinate of point plot represents the frictional pressure drop at well bottom. It can be seen from the figure that, as the steam injection velocity accelerates, the wet steam saturation pressure at annulus bottom declines, but the frictional pressure drop of wet steam is enlarged. Under a certain steam injection velocity, when the eccentricity rises, the wet steam pressure at annulus bottom increases slightly, while the frictional pressure drop is lowered slightly.

When the steam injection velocity is 35 t/d, as the eccentricity increases by 0.5, the steam frictional pressure drop declines by 1.26 kPa. If the steam injection velocity is accelerated to 50 t/d, the steam frictional pressure drop in eccentric annulus will reduce by 7.1 kPa. With the increase of steam injection velocity, the decreasing value of frictional pressure drop will rise. Combining the analytical results of the influential factors of concentric annulus steam injection parameters, we come to the conclusion that, under eccentric annular state, the influential law of mass velocity on the wellbore steam saturation pressure is identical with that of concentric annulus.

3.6. Influence of Steam Injection Outer Tube Dryness on Wet Steam Pressure at Annulus Bottom. The influence of steam injection out tube dryness on the wet steam pressure at annulus bottom is shown in Figure 14.

Figure 14 illustrates that when steam injection dryness is constant, the eccentricity rises by 0.5, and the wet steam saturation pressure at well bottom reduces by 0.02 MPa. As steam injection dryness is increased, the wet steam saturation pressure at annulus bottom significantly declines. Integrating the analytical results of influential factors of annulus steam injection dryness, under an eccentric annular structure, the influential law of steam injection dryness on wellbore steam saturation pressure is the same as that of concentric annulus.

The influence of steam injection outer tube dryness on the wet steam frictional pressure drop at annulus bottom is shown in Figure 15.

Figure 15 demonstrates that when steam injection dryness is 0.5, the eccentricity rises by 0.5, while the eccentric annulus steam frictional pressure drop falls by 0.79 kPa. As the steam injection dryness rises to 0.7, the eccentric annulus steam frictional pressure drop will decline by 7.11 kPa. The change of eccentricity has little impact on wet steam frictional pressure drop.

After comprehensively analyzing Figures 12~15, we know that when the steam injection pressure at annulus reaches an order of magnitude of 1 MPa, the eccentricity can increase from 0 to 0.5, and the steam frictional pressure drop at well bottom only changes within 0~10 kPa. Hence, the eccentricity change has little impact on steam saturation pressure at well bottom.

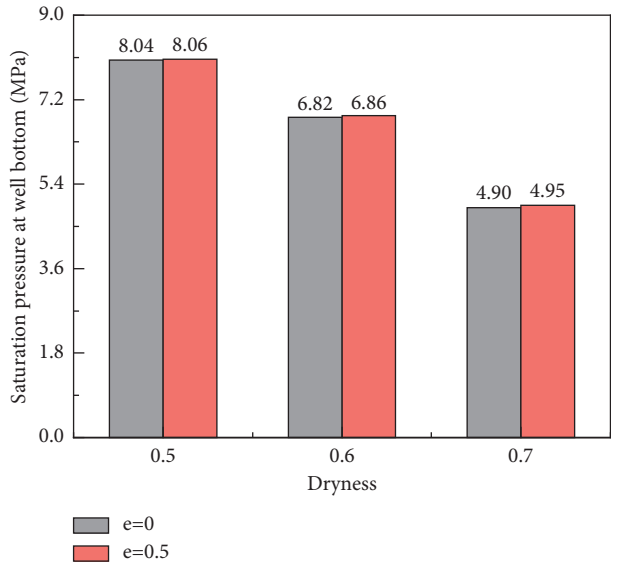

Figure 14: Influence of steam injection out tube dryness on the wet steam pressure at annulus bottom.

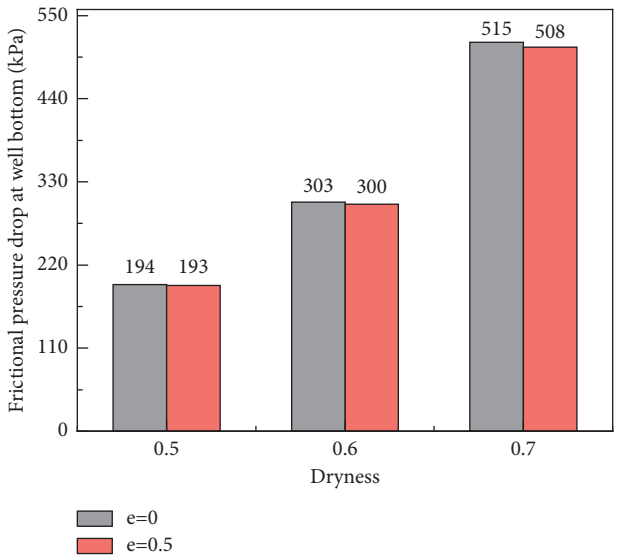

Figure 15: Influence of steam injection outer tube dryness on the wet steam frictional pressure drop at annulus bottom.

4. Conclusions

In this paper, a calculation model for steam-water two-phase flow pressure drop in vertical downward eccentric annulus was established, and a simulation calculation program was prepared. Through investigation, the influential law of the eccentricity on the steam-water two-phase flow pressure drop in vertical downward annulus was revealed, the change trend of steam on-way pressure in an annular geometric structure with eccentricity $e = 0.5$ was explored, and the accurate calculation of fully eccentric annulus liquid holdup and pressure gradient was validated. From simulation calculation, it is discovered that when the eccentricity e increases from 0 to 1, the steam frictional pressure drop at annulus bottom declines by 31.42 kPa, the saturation pressure rises by 0.265 MPa, the dryness slightly reduces by 8.54×10^{-3}, and the enthalpy value decreases by $11.22\,\mathrm{kJ \cdot kg^{-1}}$, but the wellbore heat loss is basically not affected. Therefore, we have come to the conclusion that when the steam injection pressure of dual-tube steam injection wellbore reaches an order of magnitude of 1 MPa, compared to concentrically arranged inner tube, the eccentrically arranged steam injection inner tube fails to improve the wet steam dryness at annulus bottom.

Data Availability

No data were used to support this study.

Conflicts of Interest

The authors declare that there are no potential conflicts of interest in this study.

Acknowledgments

The authors acknowledge the support from the Surface Project of National Natural Science Foundation of China (52076036) and the Northeast Petroleum University Leading Innovative Fund Project (2019YDL-12).

References

[1] R Martinezpalou, M. D Mosqueira, and B Zapatarendon, "Transportation of heavy and extra-heavy crude oil by pipeline: a review[J]," *Journal of Petroleum Science and Engineering*, vol. 75, no. 3, pp. 274–282, 2011.

[2] H. Gu, L. Cheng, S. Huang, B. Du, and C. Hu, "Prediction of thermophysical properties of saturated steam and wellbore heat losses in concentric dual-tubing steam injection wells," *Energy*, vol. 75, no. oct, pp. 419–429, 2014.

[3] F. Sun, Y. Yao, X. Li, P. Yu, L. Zhao, and Y. Zhang, "A numerical approach for obtaining type curves of superheated multi-component thermal fluid flow in concentric dual-tubing wells," *International Journal of Heat and Mass Transfer*, vol. 111, pp. 41–53, 2017.

[4] F. Sun, Y. Yao, X. Li, J. Tian, G. Zhu, and Z. Chen, "The flow and heat transfer characteristics of superheated steam in concentric dual-tubing wells," *International Journal of Heat and Mass Transfer*, vol. 115, pp. 1099–1108, 2017.

[5] F. R Sun, Y. D Yao, and X. F Li, "Numerical simulation of superheated steam flow in dual-tubing wells[J]," *Journal of Petroleum Exploration & Production Technology*, vol. 8, no. 3, pp. 1–13, 2017.

[6] F. R Sun, Y. D Yao, G Li et al., "Numerical simulation of supercritical-water flow in concentric-dual-tubing wells[C]," *America: SPE 191363-PA*, vol. 23, no. 6, pp. 1–14, 2018.

[7] X. Dong, H. Liu, Z. Pang, C. Wang, and C. Lu, "Flow and heat transfer characteristics of multi-thermal fluid in a dual-string horizontal well," *Numerical Heat Transfer, Part A: Applications*, vol. 66, no. 2, pp. 185–204, 2014.

[8] P. Li, Y. Zhang, X. Sun, H. Chen, and Y. Liu, "A numerical model for investigating the steam conformance along the dual-string horizontal wells in SAGD o," *Energies*, vol. 13, no. 15, p. 3981, 2020.

[9] Wu Han, X. Wu, and Q. Wang, "A shaft flow model of CO_2 separate injection with concentric dualtubes and its affecting factors[J]," *Acta Petrolei Sinica*, vol. 32, no. 1, pp. 723–727, 2011.
[10] H. Wang and Y. Su, "A practical method of determination of pressure loss in eccentric annulus[J]," *Oil Drilling & Production Technology*, vol. 19, no. 06, pp. 5–9, 1997.
[11] R. Ibarra, J. Nossen, and M. Tutkun, "Two-phase gas-liquid flow in concentric and fully eccentric annuli. Part I: flow patterns, holdup, slip ratio and pressure gradient," *Chemical Engineering Science*, vol. 203, pp. 489–500, 2019.
[12] R. Ibarra, J. Nossen, and M. Tutkun, "Two-phase gas-liquid flow in concentric and fully eccentric annuli. Part II: model development, flow regime transition algorithm and pressure gradient," *Chemical Engineering Science*, vol. 203, pp. 501–510, 2019.
[13] S. M. Bhagwat and A. J. Ghajar, "A flow pattern independent drift flux model based void fraction correlation for a wide range of gas-liquid two phase flow," *International Journal of Multiphase Flow*, vol. 59, pp. 186–205, 2014.
[14] V. C. Kelessidis and A. E. Dukler, "Modeling flow pattern transitions for upward gas-liquid flow in vertical concentric and eccentric annuli," *International Journal of Multiphase Flow*, vol. 15, no. 2, pp. 173–191, 1989.
[15] J. E. Julia, B. Ozar, J.-J. Jeong, T. Hibiki, and M. Ishii, "Flow regime development analysis in adiabatic upward two-phase flow in a vertical annulus," *International Journal of Heat and Fluid Flow*, vol. 32, no. 1, pp. 164–175, 2011.
[16] E. F. Caetano, O. Shoham, and J. P. Brill, "Upward vertical two-phase flow through an annulus-Part I: single-phase friction factor, taylor bubble rise velocity, and flow pattern prediction," *Journal of Energy Resources Technology*, vol. 114, no. 1, pp. 1–13, 1992.
[17] M. Wang, "The determination of overall heat transfer coefficient of isolated tubing steam injection wellbore—a supplement and discussion of the paper written by Hu Zhimian [J]," *Oil Drilling & Production Technology*, no. 6, pp. 75–78+85, 1985.
[18] E. F. Caetano, O. Shoham, and J. P. Brill, "Upward vertical two-phase flow through an annulus-Part II: m bubble, slug, and annular flow," *Journal of Energy Resources Technology*, vol. 114, no. 1, pp. 14–30, 1992.